

# The use of inverse gas chromatography to study liquid crystalline polymers\*

Marianne Romansky and James E. Guillet†

Department of Chemistry, University of Toronto, Toronto, Ontario M5S 1A1, Canada  
(Received 19 April 1993)

Liquid crystalline polymers are currently among the most widely studied classes of polymeric materials. The correlation of mesophase and liquid crystalline polymer molecular structures with observable physico-chemical properties is a major objective. In this work, inverse gas chromatography (i.g.c.) was used to determine the transition temperatures of a main chain, liquid crystalline, biphenyl-based organic polyester. The transition temperatures determined by using this method agree very well with those determined by other techniques. In addition, the i.g.c. experiment gives physico-chemical parameters for the interaction of probe molecules (saturated and aromatic hydrocarbons) with the liquid crystalline phases. Thus, enthalpies of mixing and solution of probe molecules in the polymer were estimated, and activity coefficients were calculated. From a single i.g.c. experiment, a wide range of information regarding the temperature-dependent properties of a liquid crystalline polymer was obtained.

(Keywords: inverse gas chromatography; liquid crystalline polymers; transition temperatures)

## INTRODUCTION

Liquid crystalline polymers are currently among the most widely studied classes of polymeric materials. Future advances in the field require a fundamental understanding of the solid-state structures at a molecular level. A variety of thermally stable polymers with low-temperature transitions to liquid crystal (LC) phases are presently available. The correlation of mesophase and molecular structures with observable physico-chemical properties is a major objective of the present work.

Thermotropic transitions in liquid crystalline polymers may be detected by a variety of methods, most commonly differential scanning calorimetry (d.s.c.), changes in X-ray diffraction patterns with temperature, or the observation of the texture of thin films through a polarizing light microscope.

The object of this study was to test the applicability of inverse gas chromatography (i.g.c.) to the determination of transition temperatures and physico-chemical properties of thermotropic LC polymers. In this technique, which is based on the fundamental thermodynamics of gas chromatography (g.c.), the retention behaviour of suitable probe molecules is determined as a function of temperature on columns in which the polymer is the stationary phase.

I.g.c. has been previously used to determine a variety of polymer properties<sup>1,2</sup>, including glass and other solid-phase transition temperatures, polymer melting points and degrees of crystallinity, and solution thermodynamic parameters. Recent publications<sup>3,4</sup> illustrate the wide range of applications to amorphous and semicrystalline polymer characterization. Some progress has been made in the study of macromolecular

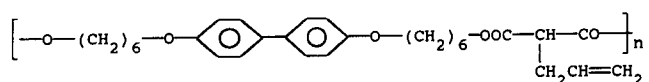
liquid crystals using i.g.c. For example, Aspler and Gray<sup>5,6</sup> have determined Flory-Huggins interaction parameters and the glass transition temperature for hydroxypropylcellulose, which forms lyotropic liquid crystalline mesophases. Nesterov *et al.*<sup>7</sup> have reported the use of i.g.c. in the detection of shallow smectic phase transitions in quinone-based polymers. On the other hand, Nishioka *et al.*<sup>8</sup> did not observe any significant deviations in probe retention times for g.c. experiments on polysiloxane side-chain liquid crystals. Martire *et al.*<sup>9</sup> and Chow and Martire<sup>10,11</sup> were the first to study in depth the interaction of very small amounts of organic solvent vapours with small-molecule liquid crystals by gas-liquid chromatography. Attempts have also been made to relate gas chromatographic data to the order of liquid crystalline phases<sup>12</sup>.

In this study, multiple transition temperatures of a liquid crystalline polyester were determined using the i.g.c. technique. The polymer chosen for this study had the thermal stability and multiple transitions necessary for the confirmation of this procedure.

## EXPERIMENTAL

### Materials

All solvents were reagent grade, and were used as received. The chromatographic support was 70/80 mesh Chromosorb G, acid-washed diatomaceous silicates deactivated with dimethyldichlorosilane (AW-DMCS). A melt condensate of diethyl allylmalonate and 4,4'-bis(6-hydroxyhexyloxy)biphenyl was prepared according to the method of Reck and Ringsdorf<sup>13</sup>, as modified by Zentel and Reckert<sup>14</sup>. The structure is shown below (I).



\* Presented at the 20th American Chemical Society National Meeting, 27 August 1992, Washington DC, USA. Published in *Proc. Am. Chem. Soc. Div. Polym. Mater. Sci. Eng.* 1992, 67, 41

† To whom correspondence should be addressed

0032-3861/94/030584-06

© 1994 Butterworth-Heinemann Ltd.

The number-average molecular weight  $M_n$ , measured by gel permeation chromatography in  $\text{CHCl}_3$  using polystyrene standards, was  $2.1 \times 10^4$ . Differential scanning calorimetry (d.s.c.) data were obtained using Perkin-Elmer DSC-2C and DSC-7 apparatus with a nitrogen purge, using heating rates of 20 and  $10^\circ\text{C min}^{-1}$ , respectively. Calibrations with indium (and decane for the DSC-7) were carried out in the usual way.

#### Inverse gas chromatography

The polymer I was deposited from  $\text{CHCl}_3$  solution onto the Chromosorb G support by the pile coating method<sup>15</sup> to a level of 5.33 wt%. A total of 0.864 g of polymer was packed into a 6.35 mm (o.d.)  $\times$  1.2 m copper tubing column. A column containing 0.372 g polymer at 2.99 wt% was also studied in order to confirm the invariance of specific retention volume with column loading. I.g.c. measurements were performed on a Hewlett-Packard 5890 Series II gas chromatograph equipped with a flame ionization detector. A precision mass flow controller with a range of 0–20 ml  $\text{min}^{-1}$  was used to control the nitrogen carrier gas at a nominal flowrate of 10 ml  $\text{min}^{-1}$ . Specific retention volumes were confirmed to be independent of the carrier flow rate at low flow rates. Barometric room pressure was measured to  $\pm 6.67$  Pa (0.05 mmHg), and column pressures were measured with a mercury manometer. Carrier gas flowrates were measured from the end of the column with a water-jacketed soap-bubble flow meter. Injections of probe vapour at infinite dilution (equivalent to  $\leq 0.01 \mu\text{l}$  of liquid), mixed with methane gas as a marker, were made from a Hewlett-Packard headspace injector (Model 19395A). Data were collected, recorded and analysed on an HP Vectra ES-12 personal computer with the associated g.c. software package HP 3365 Chemstation. The column temperature was continuously measured to  $0.1^\circ\text{C}$  with a thermocouple interfaced to the computer. The column was equilibrated for several minutes for each temperature increment of 1 or  $2^\circ\text{C}$ ; the necessary equilibration time was confirmed by the invariance of the retention times with the equilibration times. Equilibration is not necessary for transition temperature determinations; injections are usually made at intervals<sup>16–18</sup> during a heating rate of  $0.5^\circ\text{C min}^{-1}$ . However, thermal equilibration is necessary to obtain the activity coefficient data. The retention times  $t_r$  and  $t_m$  were determined from the positions of the peak maxima.

#### Calculations

Specific retention volumes  $V_g$  (ml  $\text{g}^{-1}$ ) of the probe in the polymer were computed using<sup>19</sup>

$$V_g = [F(t_r - t_m)760]/wP_o \quad (1)$$

where  $w$  is the weight of polymer in the column,  $t_r$  is the retention time of the probe,  $t_m$  is the retention time of the methane marker gas,  $F$  is the carrier gas flow rate under standard-state conditions (adjusted for gas compressibility), and  $P_o$  is the carrier gas pressure at the column outlet. Retention diagrams are plotted as the variation of  $\ln V_g$  with  $1/T$  where  $T$  is the temperature (K). The slope of the linear portions of the experimental curve is related to  $\Delta H_s^\circ$ , the heat of solution of the probe at infinite dilution in the stationary phase, by

$$\delta \ln V_g / \delta(1/T) = -\Delta H_s^\circ / R \quad (2)$$

where  $R$  is the molar gas constant. The partial molar heat of mixing, or excess enthalpy  $\Delta \bar{H}_1^\circ$ , resulting when a mole of solute is added to an infinitely large amount of polymer, is given by the change in activity coefficient with  $T$ :

$$\Delta \bar{H}_1^\circ = R[\delta \ln(a_1/w_1)^\infty] / [\delta(1/T)] \quad (3)$$

where  $(a_1/w_1)^\infty$  is the weight-fraction activity coefficient at infinite dilution of the probe in the polymer. The magnitude of  $\Delta \bar{H}_1^\circ$  indicates the extent of departure from an ideal solution.

Weight fractions and mole fractions are inter-related as follows. The mole fraction  $x_1$  is given by the number of moles of component 1,  $n_1$ , divided by the total number of moles of all of the substances in the system. For  $n_1 \ll n_2$  in a two-component system,  $x_1 \sim n_1/n_2$ . Since  $n_1 = m_1/M_1$ , where  $m_1$  is the probe mass and  $M_1$  is the probe molecular weight,  $x_1 \sim m_1 M_2 / m_2 M_1$  (after making the equivalent substitution for the polymer 2). Therefore, the weight-fraction activity coefficient of the probe in the polymer is given by  $(a_1/w_1)^\infty = \gamma_1^\infty (M_1/M_2)$ , where  $\gamma_1^\infty$  is the usual mole-fraction activity coefficient. The weight-fraction activity coefficient of the probe at infinite dilution is calculated from

$$\ln(a_1/w_1)^\infty = \ln(273R/M_1 P_1^0 V_g) - (B_{11} - V_1)P_1^0 / RT + P_o J_3^4 (2B_{13} - V_1) / RT \quad (4)$$

where  $P_1^0$  is the saturated vapour pressure at temperature  $T$ ,  $B_{11}$  is the probe virial coefficient,  $B_{13}$  is the probe-carrier gas virial coefficient, and  $J_3^4$  is a carrier-gas compressibility correction factor. These parameters may be calculated by using the methods previously reported<sup>19</sup>.  $V_1$  is the probe molar volume, calculated from the liquid molar densities at each temperature, using data from Timmermans<sup>20</sup>, Yaws<sup>21</sup>, Rackett<sup>22</sup>, and Orwoll and Flory<sup>23</sup>.

The heats of vaporization ( $\Delta H_{\text{vap}}$ ) of the probe molecules were calculated both from experimental data, where

$$\Delta H_{\text{vap}}^{\text{exp}} = \Delta \bar{H}_1^\circ - \Delta H_s^\circ \quad (5)$$

and from the relationship:

$$\Delta H_{\text{vap}}^c = M_1(d - et) \quad (6)$$

where  $d$  and  $e$  are constants which have been tabulated by Dreisbach<sup>24,25</sup>,  $t$  is the temperature (in  $^\circ\text{C}$ ) and  $M_1$  is the molecular weight of the vaporizing substance.

If the weight-fraction excess chemical potential,  ${}_w\mu^e$ , is considered,  $RT \ln(a_1/w_1)^\infty = {}_w\mu^e$  and also

$${}_w\mu^e = \Delta \bar{H}_1^\circ - T[S^e - R \ln(M_2/M_1)] \quad (7)$$

where  $S^e$  is the excess entropy. The intercept of  $\delta \ln(a_1/w_1)^\infty / [\delta(1/T)]$  gives  $[-S^e/R + \ln(M_2/M_1)]$ , and the weight-fraction excess entropy is

$${}_wS^e = S^e - R \ln(M_2/M_1) \quad (8)$$

## RESULTS AND DISCUSSION

The polyester (I) prepared for this analysis was characterized by d.s.c., X-ray diffraction, and  $^1\text{H}$  n.m.r. spectroscopy. Phase structures were confirmed by comparison of our data with data obtained for the previously synthesized<sup>14</sup> polymer. The transition temperature assignment ( $^\circ\text{C}$ ) is  $k_1$  59  $k_2$  75  $s_b$  103  $s_a$  123 i where  $k$  represents a crystal phase,  $s_a$  and  $s_b$  are the

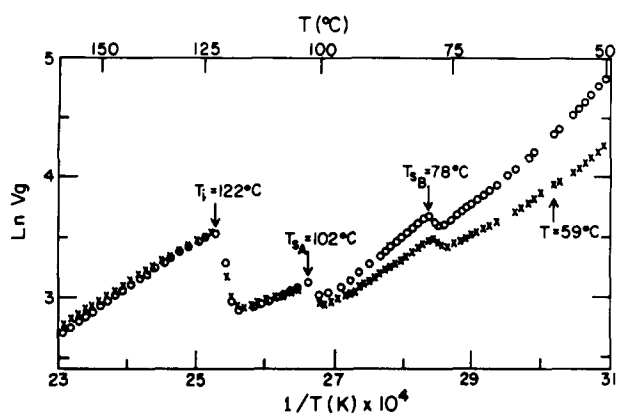


Figure 1 Retention diagrams for polymer I: (O) decane, second heating cycle and; (x) toluene, third heating cycle

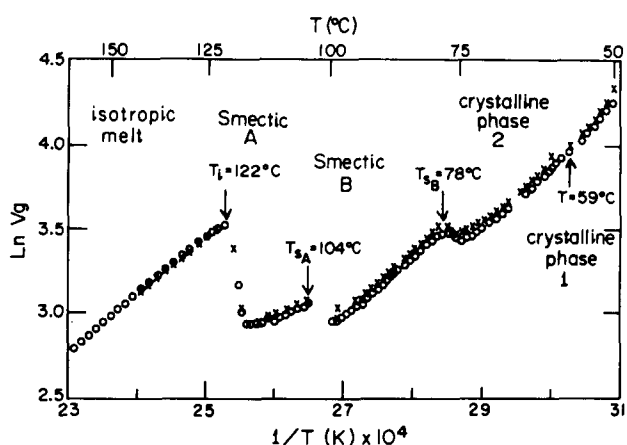


Figure 2 Retention diagrams for polymer I, using a toluene probe in duplicate isothermal experiments: (O) third heating cycle and; (x) fourth heating cycle

smectic phases A and B, and i represents the isotropic phase.

Figures 1 and 2 show i.g.c. retention diagrams for toluene and decane probes on the polymer. This biphenyl-based polyester displayed probe retention behaviour similar to that of a typical semicrystalline polymer<sup>2</sup>, with the additional feature that crystal-crystal and mesophase transitions were observed as changes in the slope below  $T_i$ , the temperature of transition to the isotropic phase. Mesophase transition temperatures were assigned to local maxima in the i.g.c. retention diagrams, corresponding to complete conversion to the higher temperature phase. This procedure was generally established for the determination of melting points in semicrystalline polymers<sup>16-18</sup>. Significantly, the determined transition temperatures were independent of the probe used (see Figure 1 for a representative example), and also of the number of preceding heating and cooling cycles. The column was slowly cooled after equilibration at 160°C (in the isotropic phase) at the end of each run. The reproducibility of the probe retention times and the specific volumes  $V_g$  on successive heating cycles after the first annealing was better than 2%. Duplicate retention diagrams for the toluene probe are illustrated in Figure 2.

The transition temperatures determined by both i.g.c. and d.s.c. are summarized in Table 1, with the temperatures listed representing the average values of several determinations for both methods. The agreement

between the two entirely different techniques is remarkable, considering that the d.s.c. scans were carried out at heating rates of 10 or 20°C min<sup>-1</sup>, whereas the i.g.c. experiments involved equilibration at successive temperatures. It may be inferred from this agreement that the chromatographic support does not influence the formation of LC phases. Our preliminary studies on this polymalonate as well as on other liquid crystalline polyesters<sup>26</sup> demonstrated a good correlation between temperature-ramped (0.5°C min<sup>-1</sup>) i.g.c. and d.s.c. measurements for the identification of transitions in LC polymers. Figure 3 shows the retention diagrams obtained for a decane probe injected manually onto the polymalonate column during a temperature ramp of 0.5°C per minute, as well as automated injections made during isothermal experiments. At low temperatures there is a significant difference between the data obtained from temperature-ramped experiments and those obtained by the equilibrium method. It is clear that thermal equilibration is necessary in order to accurately determine the heat of mixing of the probe molecule with the polymer.

The slopes of the straight-line portions of the retention diagram plots were not parallel, indicating significant differences in the entropy and enthalpy of solution of an individual probe in each of the different mesophases. Variations of the retention diagram slope in different mesophases have been observed in many g.c. experiments on small-molecule liquid crystals. Some examples are given by Kelker *et al.*<sup>27</sup> (and references cited therein).

Table 1 Thermal transitions (°C) observed for polymer I by using different techniques

Transition	I.g.c.			
	Average of isothermal runs	Temperature ramped (0.5°C min <sup>-1</sup> ) decane probe	D.s.c.	
			20°C min <sup>-1</sup>	10°C min <sup>-1</sup>
$k_1 \rightarrow k_2$	59	—	59	58
$k_2 \rightarrow s_b$	77	75	75	72
$s_b \rightarrow s_a$	102	102	103	99
$s_a \rightarrow i$	122	124 <sup>a</sup>	123	119

<sup>a</sup> Estimated value

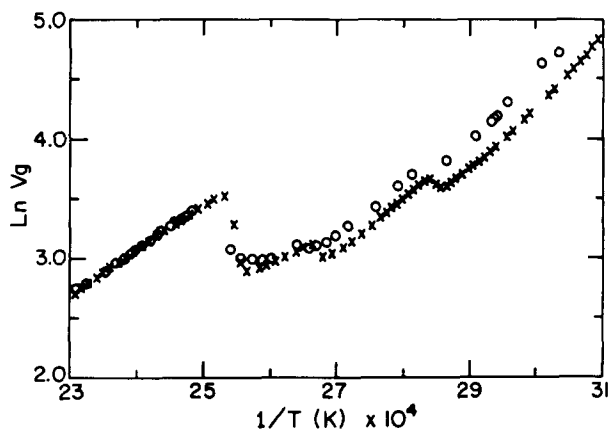


Figure 3 Retention diagrams for polymer I using an n-decane probe: (x) manual injections at a heating rate of 0.5°C min<sup>-1</sup> (first heating cycle) and; (O) automated injections under isothermal conditions (second heating cycle)

**Table 2** Partial molar enthalpies of mixing and solution ( $\text{kJ mol}^{-1}$ ) of various probes in three phases of polymer I

Probe	Isotropic		Smectic A		Smectic B	
	$\Delta\bar{H}_1^\infty$	$-\Delta H_s^\infty$	$\Delta\bar{H}_1^\infty$	$-\Delta H_s^\infty$	$\Delta\bar{H}_1^\infty$	$-\Delta H_s^\infty$
n-Decane	$11.0 \pm 0.3$	$31.7 \pm 0.2$	$23.4 \pm 0.4$	$21.7 \pm 0.3$	$8.3 \pm 0.4$	$38.9 \pm 0.3$
Toluene	$5.1 \pm 0.2$	$27.8 \pm 0.1$	$18.5 \pm 0.9$	$15.3 \pm 1.0$	$3.8 \pm 0.2$	$31.1 \pm 0.4$
<i>p</i> -Xylene	$5.1 \pm 0.2$	$31.4 \pm 0.03$	$16.6 \pm 0.1$	$21.3 \pm 0.1$	$3.6 \pm 0.2$	$32.5 \pm 0.9$
<i>m</i> -Xylene	$4.8 \pm 0.2$	$31.6 \pm 0.2$	$17.9 \pm 0.9$	$21.5 \pm 0.5$	$3.1 \pm 0.2$	$35.7 \pm 0.3$
<i>o</i> -Xylene	$4.3 \pm 0.2$	$33.1 \pm 0.03$	$19.7 \pm 0.8$	$20.9 \pm 0.4$	$3.9 \pm 0.2$	$33.5 \pm 0.1$

Enthalpies of solution,  $\Delta H_s^\infty$ , and mixing,  $\Delta\bar{H}_1^\infty$ , of the probes at infinite dilution in I are listed in Table 2. The  $\Delta H_s^\infty$  values were obtained from the slopes of the straight-line portions of the retention diagrams by using linear least-squares regression according to equation (2), and the  $\Delta\bar{H}_1^\infty$  values were similarly calculated by using equation (3)<sup>19</sup>. Due to the limited number of data points in any linear region, the enthalpies of mixing should in this case be regarded as estimates, only accurate to within  $\pm 5\%$ . Data points were selected in ranges where the correlation coefficient of a minimum of six points was at least 0.99.

The heats of solution for all of the probes were lower in the isotropic phase than in the smectic A phase, indicative of more favourable solute-solvent interactions in the higher temperature isotropic phase. Normally, solute-solvent interactions decrease at higher temperatures because of increased thermal motion. The heats of solution of the probes in the smectic B phase are much closer to the values for the isotropic phase, which may be interpreted to mean that the probe molecules are dissolving in the 'amorphous' part of the bulk phase. For example,  $\Delta H_s^\infty$  for *p*-xylene is  $-32.5 \text{ kJ mol}^{-1}$  in the smectic B phase, and  $-31.4 \text{ kJ mol}^{-1}$  in the isotropic phase. However, in the smectic A phase,  $\Delta H_s^\infty$  is  $-21.3 \text{ kJ mol}^{-1}$ .

Partial molar heats of mixing show a similar trend; high values of  $\Delta\bar{H}_1^\infty$  in the smectic A phase indicate highly non-ideal solutions, whereas the excess heats of probes with the isotropic and smectic B phases are more typical of small-molecule-polymer interactions. For *p*-xylene,  $\Delta\bar{H}_1^\infty$  in the smectic B phase (80–94°C) is  $3.1 \text{ kJ mol}^{-1}$ , in the isotropic phase (130–150°C) it is  $5.3 \text{ kJ mol}^{-1}$ , and in the smectic A phase (104–114°C) it is  $16.3 \text{ kJ mol}^{-1}$ , i.e. three times larger. This trend was manifested for all of the probes studied. The heat of mixing of n-decane is the highest in all of the phases, as would be expected since it is the least similar in its chemical structure to the polymalonate, whereas the substituted benzenes are more structurally similar to the biphenyl mesogen. For comparison, Schuster *et al.*<sup>28</sup> found a value of  $3.8 \text{ kJ mol}^{-1}$  for the  $\Delta\bar{H}_1^\infty$  of nonane in molten polystyrene at 160°C. DiPaola-Baranyi *et al.* found  $11.4 \text{ kJ mol}^{-1}$  to be the heat of mixing of decane in poly(vinyl acetate)<sup>29</sup> between 120 and 150°C, and  $13.4 \text{ kJ mol}^{-1}$  for decane in poly(methyl acrylate)<sup>30</sup> between 78 and 108°C. Experimental and calculated values of  $\Delta H_v$  derived from equations (5) and (6) are listed in Table 3 to illustrate the precision of the data on heats of mixing and solution (see Table 2). Experimental heats of vaporization are slightly higher than those calculated for the majority of probe/phase combinations, but are mostly within experimental error.

**Table 3** Experimental and calculated heats of vaporization ( $\text{kJ mol}^{-1}$ ) of various probes in three phases of polymer I

Probe	Isotropic		Smectic A		Smectic B	
	$\Delta H_v^{\text{exp}}$	$\Delta H_v^c$	$\Delta H_v^{\text{exp}}$	$\Delta H_v^c$	$\Delta H_v^{\text{exp}}$	$\Delta H_v^c$
n-Decane	42.3	42.1	45.1	45.0	47.2	47.0
Toluene	32.9	31.4	33.8	33.2	35.1	34.9
<i>p</i> -Xylene	36.5	36.4	37.9	37.8	36.1	39.1
<i>m</i> -Xylene	36.6	36.5	39.4	38.2	38.8	39.4
<i>o</i> -Xylene	37.4	37.1	40.6	39.0	37.4	40.0

The difference in the enthalpies for the different phases may be explained by a lack of penetration of the probe into the crystalline parts of a highly organized phase such as exists in the smectic B case. The concept of 'partial liquid crystallinity', proposed primarily by Lenz *et al.*<sup>31–33</sup>, has been a topic of recent discussion. Many workers reject this model on theoretical grounds, in combination with the fact that many observed biphasic systems are really a result of microheterogeneity due to molecular weight distribution and head-to-tail isomerization<sup>34</sup>. However, de Candia *et al.*<sup>35</sup> have measured the transport behaviour of gases and vapours through liquid crystalline polymers, and proposed a structure including a disordered phase within well-ordered liquid crystalline domains, based on the observed permeation. They found that isotropization enthalpies and sorption coefficients were correlated, but the diffusion coefficient was the same for different preparations of similar polymers. These findings imply a functional similarity under i.g.c. conditions to semicrystalline polymers, i.e. similar to ordered spherulites in an amorphous matrix.

The infinite-dilution partial molar excess entropy may be calculated by combining equations (7) and (8):

$$\ln(a_1/w_1)^\infty = \Delta\bar{H}_1^\infty/RT - S^e/R + \ln(M_2/M_1) \quad (9)$$

Excess entropy values for the solvents used in this study were not calculated directly, since the polymer molecular weight is not known absolutely. Rather, the weight-fraction entropy values  ${}_wS^e$  (to an accuracy of  $\pm 1\%$ ) are listed in Table 4. (However, the range of data points chosen significantly affects the intercept calculated.) All excess entropies are positive once the constant factor  $R \ln(M_2/M_1)$  is added to  ${}_wS^e$ , as in equation (8), provided that  $M_2$  is of the order of a few thousand. Weaker solute-solvent interactions in the smectic A phase (where polymer-polymer attractions are important to the stability of the mesophase) cause a predominance of the translational entropy for the solute and a high  ${}_wS^e$ . Increased solute-solvent interactions

**Table 4** Partial molar weight-fraction excess entropies ( $\text{J K}^{-1} \text{mol}^{-1}$ ) of various probes in three phases of polymer I<sup>a</sup>

Probe	Isotropic	Smectic A	Smectic B
n-Decane	2.5	27.0	-15.0
Toluene	-4.0	27.0	-14.5
<i>p</i> -Xylene	-1.9	22.2	-15.4
<i>o</i> -Xylene	-3.5	29.8	-14.3
<i>m</i> -Xylene	-3.6	24.9	-15.9

<sup>a</sup> Values are uncorrected for  $R \ln M_2/M_1$  as in equation (8)

**Table 5** Selected activity coefficients of various probes in three phases of polymer I

Probe	Smectic B		Smectic A		Isotropic	
	80°C	90°C	105°C	110°C	130°C	150°C
n-Decane	100.9	94.4	63.5	57.9	19.6	16.8
Toluene	28.4	20.4	—	11.2	5.2	4.9
<i>o</i> -Xylene	21.0	20.3	18.1	13.4	5.5	5.2
<i>p</i> -Xylene	19.3	18.7	13.7	12.9	5.8	5.6
<i>m</i> -Xylene	19.6	19.2	14.8	13.9	5.9	5.6

in the isotropic phase (i.e. reduced polymer-polymer interactions) decrease the excess entropy of the probe molecules relative to the smectic A phase. The lowest excess entropy values, in the smectic B phase, are again indicative of the more 'ideal' nature of the mixing when compared to smectic A, and may be attributed to probe solution in amorphous or non-ordered regions of the bulk polymer, as discussed above.

Activity coefficients were calculated using equation (4), and selected values are listed in Table 5. The variation of the activity coefficient with temperature (shown in Figure 4 for xylene probes) illustrates the transitions between phases as accurately as the retention diagrams. All activity coefficients show a positive deviation from Raoult's law, as expected for small molecules dissolved in polymers. The magnitudes of these coefficients are similar to values obtained for the same probes in polystyrene and poly(methyl acrylate) amorphous phases at various temperatures. DiPaola-Baranyi *et al.*<sup>29</sup> found  $(a_1/w_1)^\infty$  for decane in poly(vinyl acetate) at 135°C to be 38.0. Schuster *et al.*<sup>28</sup> found a weight fraction activity coefficient of 4.87 for toluene in molten polystyrene at 140°C, and 9.94 for nonane at 130°C. In the case of small-molecule liquid crystals, Coca *et al.*<sup>36</sup> found an activity coefficient of 1.846 for toluene in the smectic phase of 4,4'-bis(heptyloxy)azoxybenzene at 80°C. Calculations based on their published data yield a weight-fraction activity coefficient of approximately 8.9. In the isotropic phase at 130°C, an activity coefficient of 0.794 can be converted into a weight-fraction activity coefficient of 3.7.

The activity coefficient of the *p*-xylene isomer is significantly lower than that of the other two isomers in the liquid crystalline phases, but not in the isotropic phase. Similar observations have been made in g.c. studies of small-molecule stationary phases<sup>10,11,27,37</sup>. The interpretation of the relationship between activity coefficients and the extent of order is not yet clear, since the influence of the anisotropic environment<sup>37</sup> is not accounted for in the regular solution theory on which the calculation of enthalpies is based.

The rationale behind the use of activity coefficients derives from some concepts introduced by Humphries *et al.*<sup>38</sup>. An orientation-dependent activity coefficient  $\gamma_{or}^\infty$  may be introduced, since the main difference in the activity coefficients at the transition between a liquid crystal ( $\gamma_a^\infty$ ) and an isotropic phase ( $\gamma_i^\infty$ ) is due to the orientational free energy.

$$\ln \gamma_{or}^\infty = \ln \gamma_a^\infty - \ln \gamma_i^\infty \quad (10)$$

When modelled for a simple small-molecule nematic phase, using the Maier-Saupe order parameter prediction of 0.4292 at the nematic to isotropic transition, an orientational (mole-fraction) activity coefficient  $\gamma_a^\infty/\gamma_i^\infty$  of 1.5 is predicted<sup>27</sup>. A nearly constant value of 1.1 has been found for g.c. experiments involving the solution of hydrocarbons in small-molecule nematic liquid crystals<sup>11,27,37</sup>. The correlation is significant for this rather unrefined theory.

The ratio of the activity coefficients  $\gamma_{or}^\infty$  for all probes studied in the smectic A phase to those in the isotropic phase is approximately 2.0; for the smectic B-smectic A transition, the respective activity coefficient ratio is approximately 1.2. These ratios were calculated by linearly extrapolating the  $\ln(a_1/w_1)^\infty$  values to the inflection point in plots such as the ones shown in Figure 4, and calculating the hypothetical activity coefficients in each phase at the transition temperature. The error in these determinations is  $\pm 0.1$ , since the selection of the actual transition point will affect the activity coefficient values that are found. The activity coefficients tabulated in Table 5 illustrate the decrease in activity coefficient with an increase in both temperature and molecular disorder. Experiments are in progress on a variety of LC polymers to systematize and expand on the trends that have been observed.

## CONCLUSIONS

Inverse gas chromatography is a powerful tool in the determination of transition temperatures of thermotropic liquid crystalline polymers. Polymer LC phase transitions found by i.g.c. correlate well with those obtained by d.s.c. measurements. In situations where d.s.c. experiments

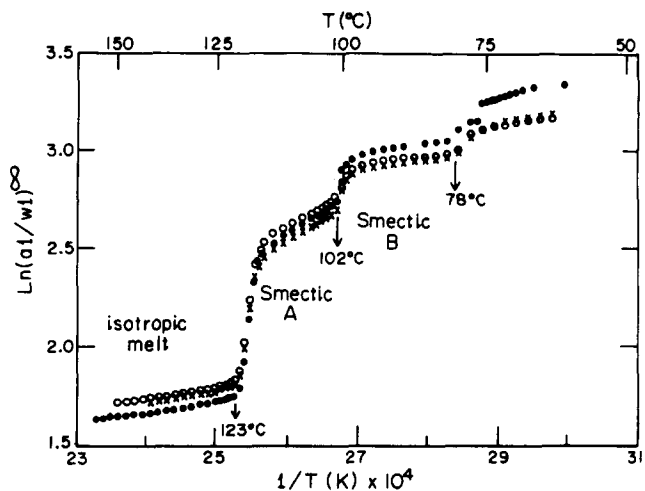


**Figure 4** Variation in the activity coefficient with temperature for xylene isomer probes, where the marked temperatures correspond to the transition temperatures, obtained from the corresponding i.g.c. retention diagrams: (●) *o*-xylene (seventh heating cycle); (○) *p*-xylene (eighth heating cycle) and; (×) *m*-xylene (ninth heating cycle)

may produce poorly resolved peaks, or where X-ray determinations are unavailable, i.g.c. can be an important experimental adjunct. In addition, a thermodynamic description of the interaction of small molecules with LC phases can be obtained. Data in this category are of prime importance to both industrial and academic research for the comprehension and design of blends of liquid crystalline polymers with small molecules or polymers, and chemical reactions in LC phases, as well as the properties of the LC polymers themselves.

#### ACKNOWLEDGEMENTS

Mr Holger Poths (University of Mainz) kindly performed the X-ray measurements. Some synthesis and characterization was carried out (by M. R.) in the laboratories of Professor H. Ringsdorf and Dr R. Zentel at the University of Mainz. We thank the Natural Sciences and Engineering Research Council of Canada for financial support of this work, and The Ontario Centre for Materials Research for an equipment grant to purchase the Hewlett-Packard gas chromatography system.

#### REFERENCES

- Conder, J. R. and Young, C. L. 'Physicochemical Measurements by Gas Chromatography', Wiley, New York, 1979
- Lipson, J. E. and Guillet, J. E. in 'Developments in Polymer Characterisation - 3' (Ed. J. V. Dawkins), Applied Science, Barking, 1982
- 'Inverse Gas Chromatography' (Eds D. R. Lloyd, T. C. Ward and H. P. Schreiber), ACS Symposium Series 391, American Chemical Society, Washington, DC, 1989
- Orts, W. J., Romansky, M. and Guillet, J. E. *Macromolecules* 1992, **25**, 949
- Aspler, J. S. and Gray, D. G. *Macromolecules* 1979, **12**, 562
- Aspler, J. S. and Gray, D. G. *Polymer* 1982, **23**, 43
- Nesterov, V. V., Turkova, L. D., Shepelevskii, A. A. and Belen'kii, B. G. *Vysokomol. Soedin. Ser. B* 1983, **25**, 630
- Nishioka, M., Jones, B. A., Tarbet, B. J., Bradshaw, J. S. and Lee, M. L. *J. Chromatogr.* 1986, **357**, 79
- Martire, D. E., Blasco, P. A., Carone, P. F., Chow, L. C. and Vicini, H. *J. Phys. Chem.* 1968, **72**, 3489
- Chow, L. C. and Martire, D. E. *J. Phys. Chem.* 1969, **73**, 1127
- Chow, L. C. and Martire, D. E. *J. Phys. Chem.* 1971, **75**, 2005
- Zheng, G., Zhou, X. and Li, P. *Thermochim. Acta* 1990, **169**, 301
- Reck, B. and Ringsdorf, H. *Makromol. Chem. Rapid Commun.* 1985, **6**, 291
- Zentel, R. and Reckert, G. *Makromol. Chem.* 1986, **187**, 1915
- Al-Saigh, A. Y. and Munk, P. *Macromolecules* 1984, **17**, 803
- Guillet, J. E. and Stein, A. N. *Macromolecules* 1970, **3**, 102
- Stein, A. N., Gray, D. G. and Guillet, J. E. *Br. Polym. J.* 1971, **3**, 175
- Gray, D. G. and Guillet, J. E. *Macromolecules* 1971, **4**, 129
- Braun, J. E. and Guillet, J. E. *Macromolecules* 1977, **10**, 101
- Timmermans, J. 'Physico-Chemical Constants of Pure Organic Compounds', Vol. 2, Elsevier, New York, 1965
- Yaws, C. L. *Chem. Eng.* 1975, 113
- Rackett, H. G. *J. Chem. Eng. Data* 1970, **15**, 514
- Orwoll, R. A. and Flory, P. J. *J. Am. Chem. Soc.* 1967, **89**, 6814
- Dreisbach, D. *Adv. Chem. Ser.* 1959, **22**, 4
- Dreisbach, D. *Adv. Chem. Ser.* 1959, **33**, 56
- Romansky, M. and Guillet, J. E. 33rd IUPAC International Symposium on Macromolecules, Montreal, Canada, July 1990
- Kelker, H., Hatz, R. and Schumann, C. (Eds) 'Handbook of Liquid Crystals', VCH, Weinheim, 1980, Ch. 9
- Schuster, R. H., Gräter, H. and Cantow, H.-J. *Macromolecules* 1984, **17**, 619
- DiPaola-Baranyi, G., Guillet, J. E., Jeberien, H. E. and Klein, J. *Makromol. Chem.* 1980, **181**, 215
- DiPaola-Baranyi, G. and Guillet, J. E. *Macromolecules* 1978, **11**, 224
- Rami Reddy, C. and Lenz, R. W. *J. Polym. Sci., Polym. Chem. Edn* 1991, **29**, 1015
- Lenz, R. W. *Faraday Discuss. Chem. Soc.* 1985, **79**, 21
- Lenz, R. W., Rao, A. K., Rami Reddy, C., Bafna, S. and Bhattacharya, S. J. *J. Polym. Sci., Polym. Phys. Edn* 1989, **27**, 2117
- Martin, P. G. and Stupp, S. I. *Macromolecules* 1988, **21**, 1222
- de Candia, F., Capodanno, V., Renzulli, A. and Vittoria, V. *J. Appl. Polym. Sci.* 1991, **42**, 2959
- Coca, J., Medina, I. and Langer, S. H. *Chromatographia* 1988, **25**, 825
- Oweimreen, G. A., Lin, G. C. and Martire, D. E. *J. Phys. Chem.* 1979, **83**, 2115
- Humphries, R. L., James, P. G. and Luckhurst, G. R. *Symp. Faraday Soc.* 1975, **5**, 107